

Supplementary Information

New insights into radial structural differences of polyacrylonitrile fibres during thermal stabilization by the synchronous processing adjustment of time and temperature

Liang Chen^{a, c, 1}, *Jing Chen*^{a, 1}, *Zhigang Shen*^{c, **}, *Jie Liu*^{a, b}, *Xiaoxu Wang*^{a, b, *}

a Key Laboratory of Carbon Fiber and Functional Polymers, Ministry of Education, Beijing University of Chemical Technology, Chao-Yang District, Beijing 100029, China

b Changzhou Institute of Advanced Materials, Beijing University of Chemical Technology, Changzhou, Jiangsu 213164, China.

c Shanghai Research Institute of Petrochemical Technology, Pudong New District, Shanghai, 201211, China.

1 Both authors equally contributed to this work.

Correspondence to:

*: *Xiaoxu Wang* (E-mail: wangxiaoxu@mail.buct.edu.cn)

** : *Zhigang Shen* (E-mail: shenzg.sshy@sinopec.com)

3. Results and discussions

3.1 Methodology

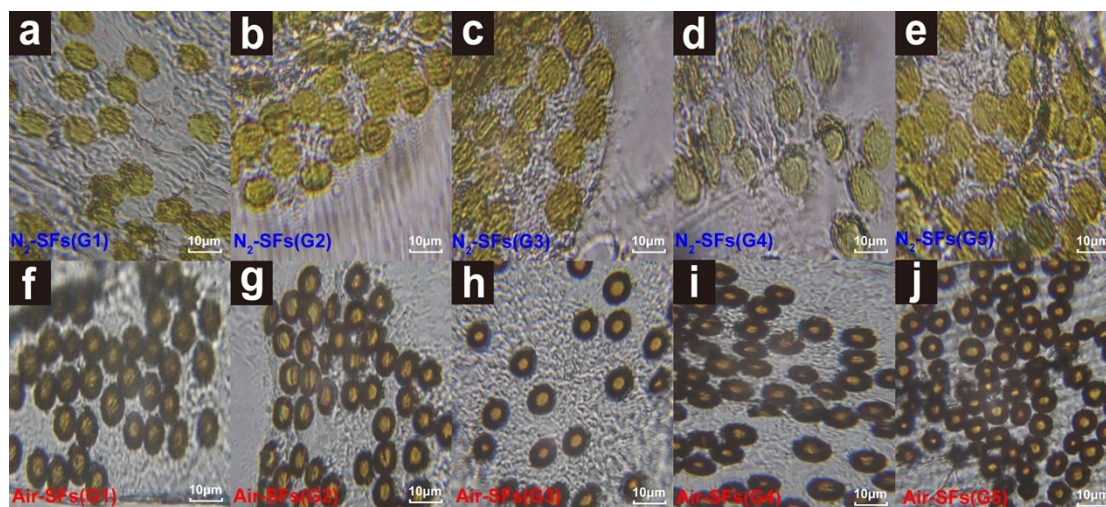


Fig. S1 Optical images of the fibers' cross sections of Air-SFs and N_2 -SFs obtained by several TTI adjustments, including (a) Air-SFs(G1), (b) Air-SFs(G2), (c) Air-SFs(G3), (d) Air-SFs(G4), and (e) Air-SFs(G5); (f) N_2 -SFs(G1), (g) N_2 -SFs(G2), (h) N_2 -SFs(G3), (i) N_2 -SFs(G4), and (j) N_2 -SFs(G5).

Table S1 The detailed results of relative element contents, including C, N, and O, of the linear testing points of Air-SFs(G3) and N_2 -SFs(G3). All the results below are recorded by SEM-EDS test.

	Testing points code	Air-SFs			N_2 -SFs		
		C	N	O	C	N	O
Relative element contents (wt%)	1	72.19	17.97	9.84	74.12	19.93	5.95
	2	65.30	28.78	5.92	72.73	21.54	5.73
	3	65.21	28.82	5.97	71.43	22.58	5.99
	4	64.28	29.65	6.07	68.62	25.57	5.81
	5	61.98	27.96	10.06	73.60	20.33	6.07
	/	100 wt% in total			100 wt% in total		

Air-SFs(G3)

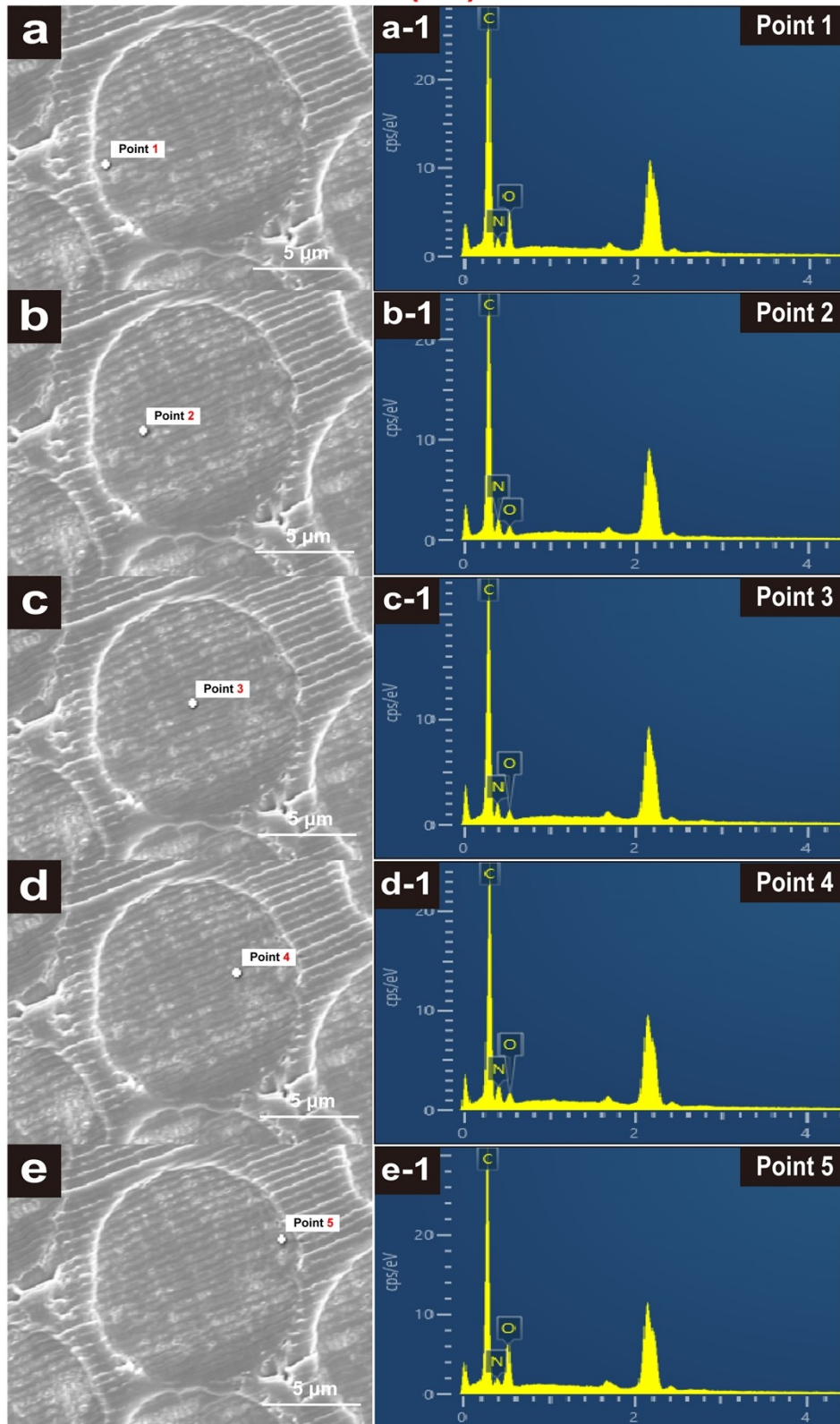


Fig. S2 SEM images and energy dispersive spectra of Air-SFs during several TTI adjustments, including (a) Air-SFs(G1), (b) Air-SFs(G2), (c) Air-SFs(G3), (d) Air-SFs(G4), and (e) Air-SFs(G5).

N_2 -SFs(G3)

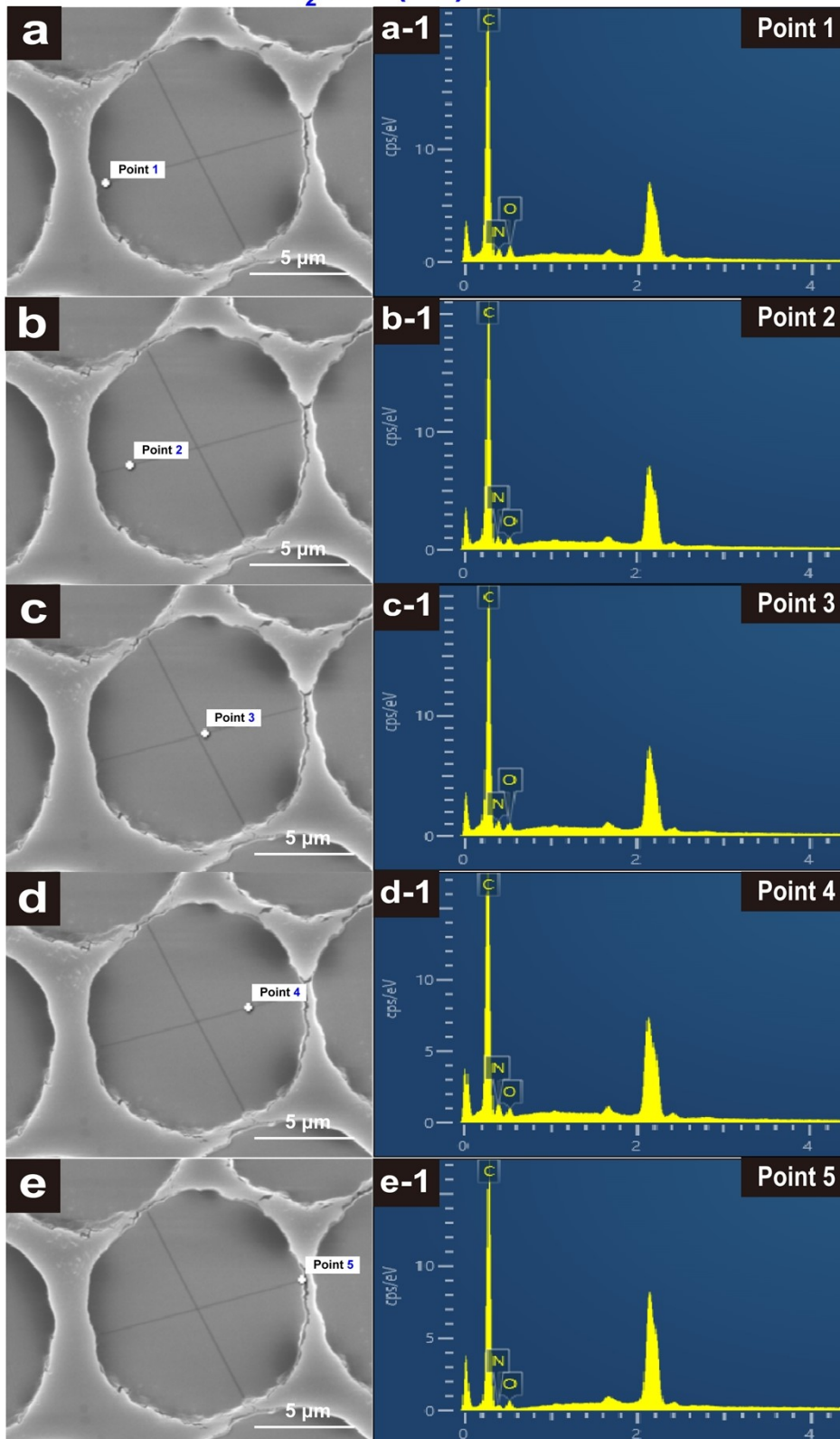


Fig. S3 SEM images and energy dispersive spectra of N_2 -SFs during several TTI adjustments, including (a) N_2 -SFs(G1), (b) N_2 -SFs(G2), (c) N_2 -SFs(G3), (d) N_2 -SFs(G4), and (e) N_2 -SFs(G5).

3.2 The integrating effects of time/temperature on the stabilization/aggregation structures parameters both in the skin and core regions of stabilized PAN fibers

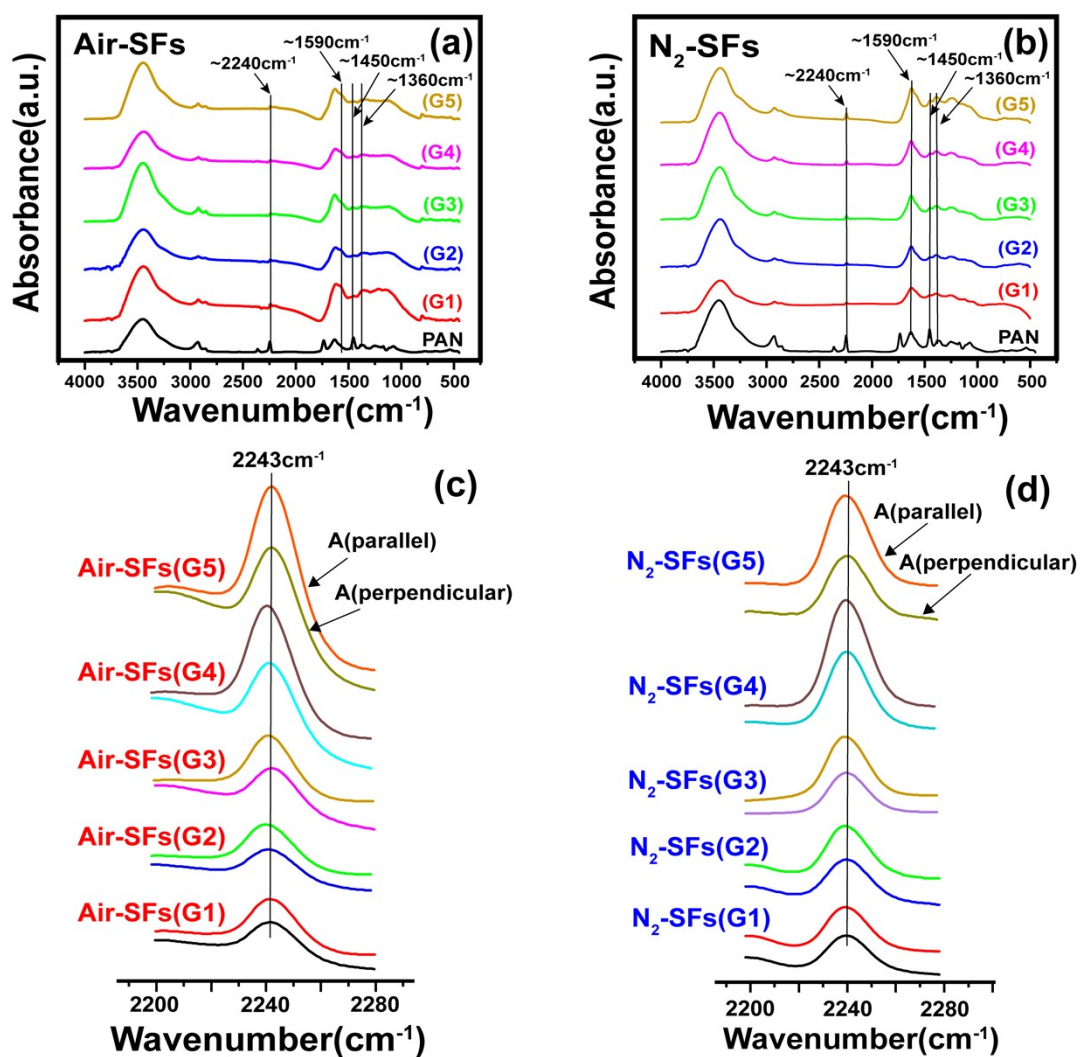


Fig. S4 FTIR spectra of several stabilized PAN fibers, (a) Air-SFs from G1 to G5, (b) N_2 -SFs from G1 to G5; (c) polarized FTIR spectra obtained by parallel and perpendicular directions for each stabilized PAN fibers sample, (c) Air-SFs from G1 to G5, (d) N_2 -SFs from G1 to G5.

Table S2 Detailed orientation degrees of PAN chains both in skin and core regions of Air-SFs samples. The values of ' FNs_{core} ' and ' DHI_{core} ' are obtain by measuring overall fraction of reacted nitrile groups and the orientation degree in quasicrystals of N_2 -SFs, respectively.

Name	FNs (%)	FNs_{skin} (%)	FNs_{core} (%)	DHI (%)	DHI_{skin} (%)	DHI_{core} (%)
------	-----------	---------------------	---------------------	--------------	---------------------	---------------------

PAN	11.50	/	/	0.5847	/	/
Air-SFs (G1)	82.86	84.82	75.40	5.7037	6.5627	2.4348
Air-SFs (G2)	80.65	82.24	73.82	3.9619	4.3415	2.3103
Air-SFs (G3)	77.53	79.01	70.56	1.3469	1.3002	1.5682
Air-SFs (G4)	79.54	81.45	70.32	2.8421	3.0629	1.4902
Air-SFs (G5)	81.33	83.92	68.73	3.1579	3.4188	1.4253

Table S3 Evolutions of modified aggregation structures both in the skin and core regions of Air-SFs. The values of ' L_c ', ' β_{core} ', ' $L_{c, core}$ ' and ' $\beta_{c, core}$ ' are obtain by measuring overall crystalline size, crystallinity, crystalline size of N_2 -SFs, and crystallinity of N_2 -SFs, respectively.

Name	η	β (%)	β_{core} (%)	β_{skin} (%)	L_c (nm)	$L_{c,core}$ (nm)	$L_{c,skin}$ (nm)
PAN	0	56.23	/	/	7.4473	/	/
Air-SFs (G1)	0.7923	17.98	34.21	13.71	1.3772	1.8269	1.2591
Air-SFs (G2)	0.8033	20.18	35.68	16.61	1.4694	2.0225	1.3422
Air-SFs (G3)	0.8252	23.21	44.29	18.76	1.5032	2.2176	1.3526
Air-SFs (G4)	0.8331	20.61	44.95	16.63	1.4808	2.2225	1.3596
Air-SFs (G5)	0.8420	19.17	45.32	15.23	1.4771	2.3181	1.3504

3.3 The integrating effects of time/temperature on the orientation of PAN chains

both in the skin and core regions of stabilized PAN fibers

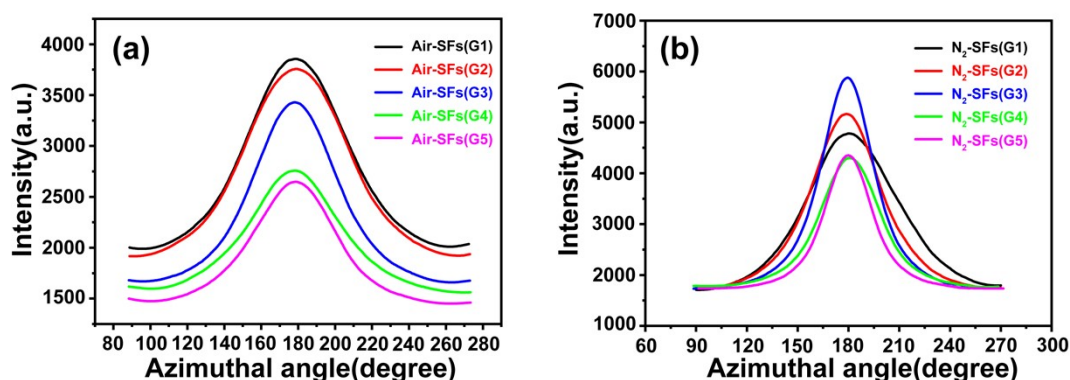


Fig. S5 Azimuthal scans at $2\theta=16.7^\circ$ of XRD pattern of stabilized PAN fibers sample with different TTIs. (a) Air-SFs from G1 to G5, and (b) N_2 -SFs from G1 to G5. Where the N_2 -SFs is considered as core structure of Air-SFs based on the mathematic model.

Table S4 Detailed orientation degrees of PAN chains both in skin and core regions of Air-SFs samples. The values of ' f_{core} ' and ' $f_{c,core}$ ' are obtain by measuring overall orientation degree and the

orientation degree in quasicrystals of N₂-SFs, respectively.

Name	f	f_c	f_a	f_{core}	f_{skin}	$f_{c,core}$	$f_{c,skin}$	$f_{a,core}$	$f_{a,skin}$
PAN	0.5523	0.8291	0.2549	/	/	/	/	/	/
Air-SFs (G1)	0.3088	0.6467	0.2347	0.1993	0.3375	0.6557	0.6443	0.0287	0.2888
Air-SFs (G2)	0.3566	0.7119	0.2668	0.2276	0.3882	0.7347	0.7066	0.0301	0.3248
Air-SFs (G3)	0.3588	0.7327	0.2458	0.2919	0.3730	0.7861	0.7214	0.0254	0.2925
Air-SFs (G4)	0.4121	0.7248	0.3309	0.3521	0.4241	0.7775	0.7161	0.1565	0.3659
Air-SFs (G5)	0.4124	0.6959	0.3452	0.3809	0.4183	0.8145	0.6781	0.2041	0.3716

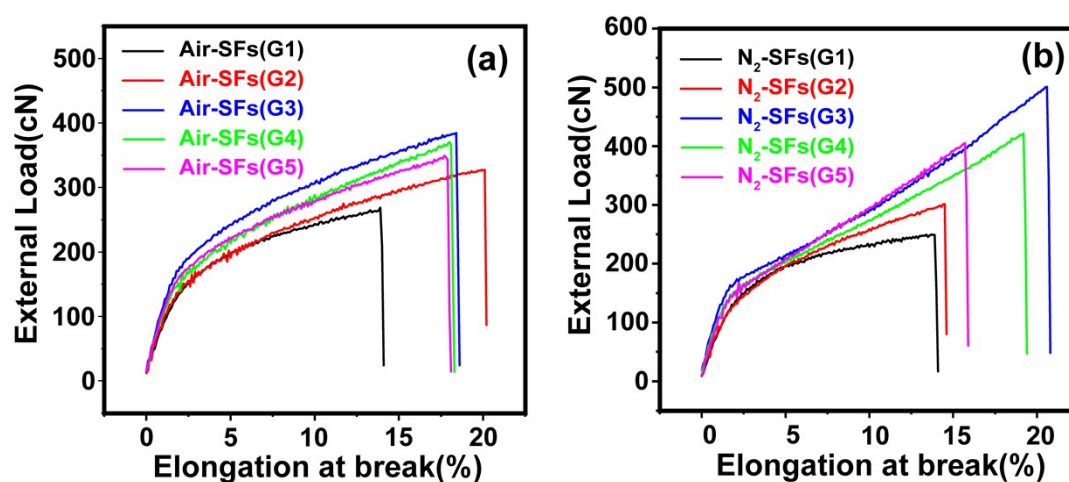


Fig. S6 Stress-strain curves of (a)Air-SFs from G1 to G5, and (b)N₂-SFs from G1 to G5.

Table S5. The details of mechanical properties of several stabilized PAN fibers, including that (a) Air- SFs from G1 to G5, and (b) N₂-SFs from G1 to G5.

Sample code	T.S. (GPa)	CV (%)	T.M. (GPa)	CV (%)
Air-SFs (G1)	262.1	7.1	9236.6	20.6
Air-SFs (G2)	330.5	8.2	10744.9	27.5
Air-SFs (G3)	384.2	9.5	12280.2	26.7
Air-SFs (G4)	368.4	9.8	12983.5	38.7
Air-SFs (G5)	349.5	7.3	12903.1	31.8
N ₂ -SFs (G1)	295.1	6.1	8257.9	16.3
N ₂ -SFs (G2)	367.4	7.2	10436.7	23.4
N ₂ -SFs (G3)	459.4	4.2	11393.1	31.4
N ₂ -SFs (G4)	422.8	8.4	11956.3	33.6
N ₂ -SFs (G5)	401.2	7.5	12724.7	34.8

3.4 The effects of the stabilized PAN fibers' structural differences on the resultant carbon fibers performances

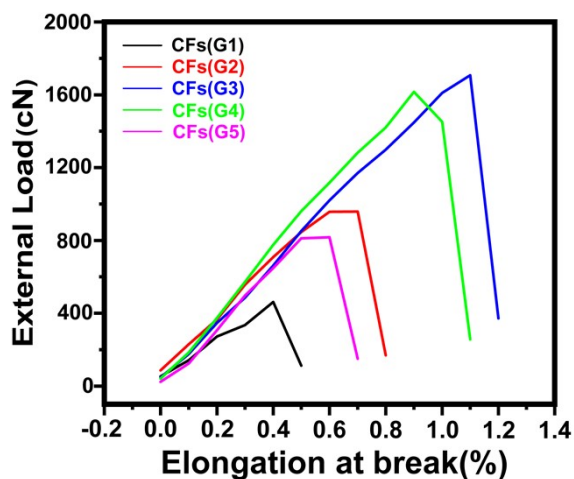


Fig. S7 Stress-strain curves of the resultant CFs from G1 to G5.

Table S6 Mechanical properties of the resultant carbon fibers from G1 to G5, including tensile strength, tensile modulus and elongation at break.

Sample code	T.S. (MPa)	CV (%)	T.M. (GPa)	CV (%)	ϵ (%)	CV (%)
CFs(G1)	530.7	5.8	128.9	20.4	0.6	8.4
CFs(G2)	946.6	6.3	132.8	23.5	0.8	14.9
CFs(G3)	1720.8	10.4	179.4	19.8	1.1	10.3
CFs(G4)	1527.1	7.5	193.6	18.5	1.0	9.2
CFs(G5)	1128.3	9.6	192.5	16.4	0.7	11.4

Table S7 D/G ratio (I_D/I_G) and graphite stack thickness (L_c) of the resultant carbon fibers (CFs) from G1 to G5.

Sample code	I_D/I_G	L_c (nm)
CFs(G1)	0.9454	1.11
CFs(G2)	0.9168	1.09
CFs(G3)	0.8536	1.39
CFs(G4)	0.8975	1.32
CFs(G5)	0.9084	1.27

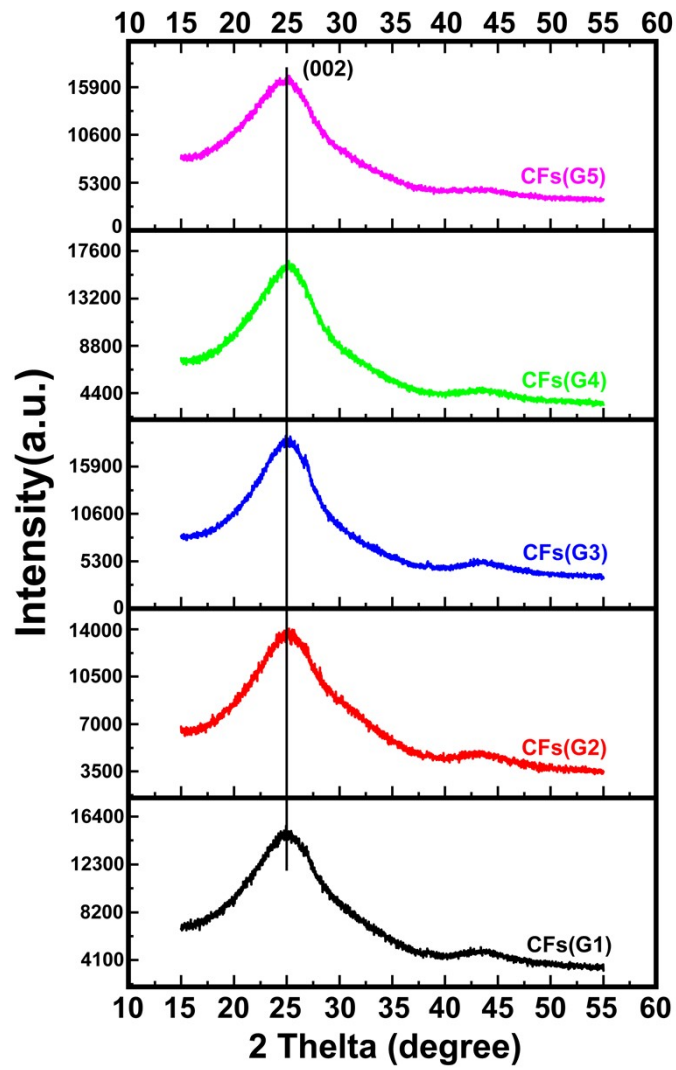


Fig. S8 Stack plot of XRD patterns of carbon fiber samples from G1 to G5.